

Structural design of 3-dimensional disk electrode based on Cu-CoO composite for Li-ion battery

Cheol-Woo Ahn*, Young-Hoon Chung**, Byung-Dong Hahn*, Dong-Soo Park*, and Yung-Eun Sung**[†]

*Functional Ceramics Group, Korea Institute of Materials Science (KIMS), Changwon, Gyeongnam 641-831, Korea

**School of Chemical & Biological Engineering & Research Center for Energy Conversion and Storage,
Seoul National University, Seoul 151-744, Korea

(Received 17 June 2011 • accepted 2 November 2011)

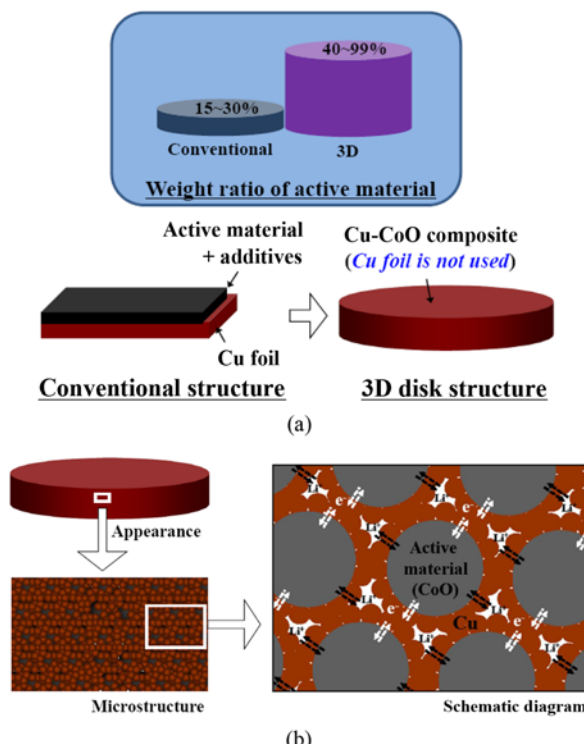
Abstract—A 3-dimensional disk electrode structure was designed to further improve the capacity and reduce the weight in the anode of a Li-ion battery. The additives, such as binding and carbon based conducting materials, were removed. In particular, Cu foil was not used in this 3-dimensional disk electrode. All the specimens were fabricated using conventional ceramic process, which was appropriate for the scale-up in industry. In the 3-dimensional disk electrode, the Cu-CoO composite was selected and excellent capacity was observed.

Key words: Ceramic Composites, Porous Materials, Composite Materials

INTRODUCTION

Regarding the Li-ion battery, many studies have been conducted to enhance its electrochemical capability especially in active mate-

rials such as oxides, composites etc. [1-14]. However, these developments have been limited to the design of active materials. Thus, we designed a new electrode structure, which is the structure for not active material but electrode, in order to obtain further improve-



Scheme 1. 3D disk electrode structure designed in this study: (a) structure difference between conventional electrode and 3D disk electrode, (b) appearance, microstructure, and schematic diagram of 3D disk electrode, and (c) F and C2 as a function of particle size ratio (between Cu and CoO) in the 3D disk electrode (Inset: F and C2 variations with Cu particle sizes in 3D disk electrode, when the particle size of CoO is 1 μm).

[†]To whom correspondence should be addressed.

E-mail: ysung@snu.ac.kr

ment in capacity by increasing the weight ratio of active material at the electrode as indicated in Scheme 1. It was achieved by removing additive materials and, especially, Cu foil. Furthermore, this electrode structure is good for lightening the weight of the Li-ion battery. The total weight of electrode is reduced by removing the additive materials. The conventional ceramic process was chosen, considering the scale-up in industry.

To clarify the excellent quality of 3-dimensional (3D) disk electrode in capacity, the capacity must be calculated by using the weight of not only active material (C1) but also the whole electrode (C2). The aim of this work is the C2 improvement and light weight pf the electrode of the Li-ion battery. Hence, in this study, the fraction of active material (F, wt%) must be considered as the following:

$$F = \frac{\text{active material}}{\text{active material} + \text{conducting material} + \text{binder} + \text{Cu foil}} \quad (1)$$

Primarily, F means the weight ratio of active material in anode. It must be investigated to clarify the benefit of 3D disk structure as seen in Table 1, since C2 can be calculated by:

$$C_2 = C_1 \cdot F \quad (2)$$

To lighten the electrode weight, F and C2 must be improved. In a typical electrode structure, F magnitude might be located at around 0.15-0.30 region (due to the Cu foil and additives, especially Cu foil), which is lower than that of 3D disk structure as seen in Scheme 1 and Table 1. The thickness of Cu foil was assumed to be 20-30 μm

Table 1. Calculated capacities of typical and 3D disk structure for the anode in Li-ion battery: It was supposed that F might be around 15-30 wt% in typical electrode structure, owing to the large fraction of Cu foil as well as the other additives such as binding and carbon based conducting materials. They were calculated using the weight of not only active material (C1) but also whole electrode (C2)

	Typical electrode		3D disk electrode	
	Graphite	CoO	40 wt% CoO	90 wt% CoO
F [wt%]	15-30	15-30	40	90
C1 [mAh g ⁻¹]	372	715	715	715
C2 [mAh g ⁻¹]	56-112	107-214	286	643

and its reduction might be under trial at many companies. Because of low F, the conventional structure can show relatively low C2, compared to the 3D disk electrode as shown in Table 1. Moreover, C2 of the 3D disk electrode can be controlled by the particle size ratio as shown in Scheme 1(c). F and C2 magnitudes of 3D disk structure in Table 1 and Scheme 1(c) were calculated on the assumption that the surface of every CoO particle was entirely covered with one layer of Cu particles, and all of the CoO particles completely functioned for active materials in 3D disk electrode as shown in the diagram of Scheme 1(b). Since the particle size of the active material must be large to obtain high F, CoO was chosen to assemble the 3D disk electrode in this work. It has been reported that the CoO

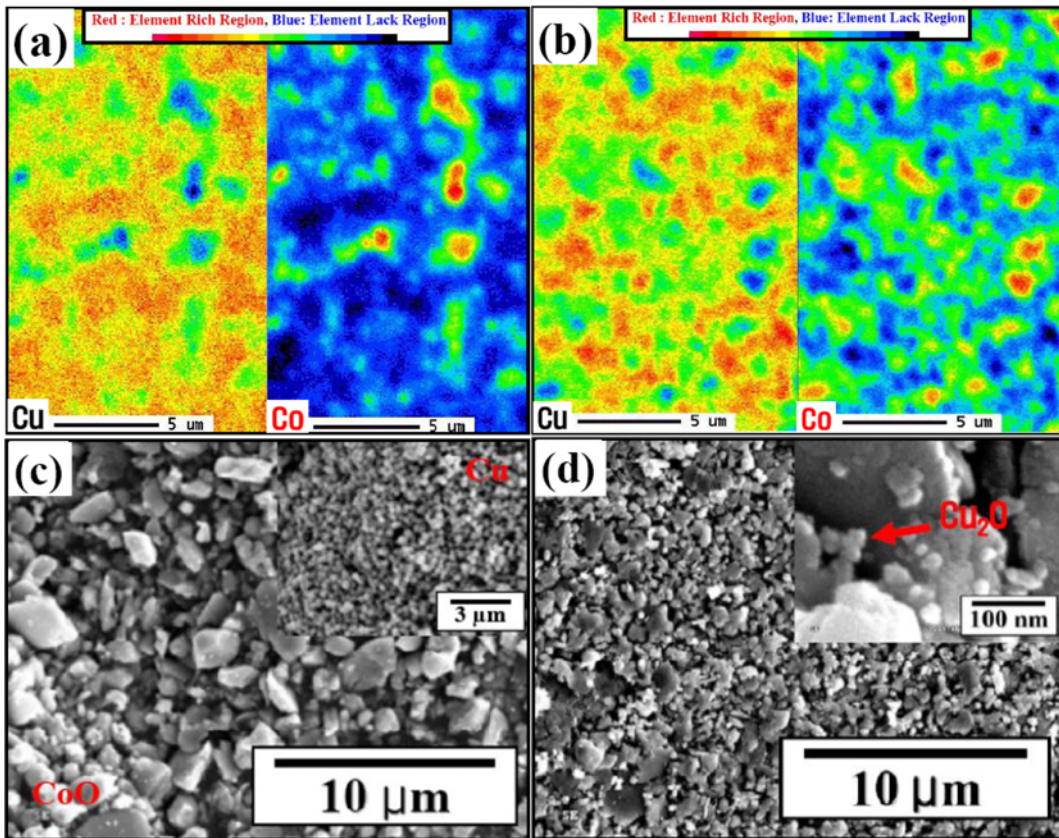


Fig. 1. EPMA images of (a) 0.1 and (b) 0.4 3D disk electrodes sintered at 500 and 600 °C for 2 h in N₂ atmosphere and SEM [field emission scanning electron microscopy (FE-SEM): Hitachi S-4300, Tokyo, Japan] images of (c) raw powders and (d) 0.4 3D disk electrode sintered at 600 °C in N₂ atmosphere.

CoO [particle size $\sim 1 \mu\text{m}$, Fig. 1(c)] and Cu [$\sim 300 \text{ nm}$, Fig. 1(d)] powders were chosen to assemble the 3D disk electrode. Two compositions of 0.6 Cu - 0.4 CoO (at weight ratio, 0.4 3D disk electrode) and 0.9 Cu - 0.1 CoO (0.1 3D disk electrode) were prepared and compared to each other in this study. The composition of 0.4 3D disk electrode was chosen by considering the F value as seen in Scheme 1(c), and 0.1 3D disk electrode was selected because it has similar C2 to graphite-based conventional electrode. The 3D disk electrode was prepared by using the typical ceramic process which is suitable for scale-up in industry [15]. CoO and Cu powders were ball-milled for 4 h and compacted under a pressure of 100 kg/cm^2 . They were sintered at the range of $500\text{-}600^\circ\text{C}$ for 2 h in N_2 atmosphere. Coin-type cells (CR 2016) were assembled in an argon-filled glove box. The prepared 3D disk electrode and a metallic lithium foil were used as the working electrode and the counter electrode. A 1 M LiPF₆ [a mixture of ethylene carbonate (EC) and dimethyl carbonate (DMC) (1 : 1 volume ratio)] was used as the electrolyte and a polypropylene (pp) film (Celgard 2400) was chosen for the separator. The cells were cycled by using a multi-channel battery cycler (Toyo System Co., Ltd.) between 0.001 V and 3.000 V at a rate of C/5.

To confirm the formation of Cu-CoO composite and the distribution of particles, an electron probe X-ray micro-analysis (EPMA: JXA-8900R, JEOL, Japan) was carried out as shown in Figs. 1(a)-(b). The regions of CoO and Cu were clearly distinguished, and the trends of their levels and areas were completely opposite. Therefore, it was expected that Cu-CoO composites were well-formed and CoO particles were well-distributed among Cu particles. However, the oxidation of Cu was also detected by EPMA as shown in Table 2. There was a gap in the oxidation ratio of Cu, since Co is oxidized more easily than Cu, as found at the Ellingham diagram [16,17]. The good formation of the Cu-CoO composite was confirmed by XRD patterns at which no other peak was found at 0.1 and 0.4 3D disk electrodes except CoO, Cu, and Cu₂O peaks (not shown in this manuscript).

The particle sizes were investigated because it has been well-known that the particle size is an important factor in the electrochemical behavior of Cu₂O, although it does not show a significant effect on the capacity of CoO [14]. Fig. 1(d) shows the porous microstructure (density=76.3%, measured by the Archimedes method.) of 0.4 3D disk electrode specimen. Quite small particles (Cu₂O, 10-25 nm) were observed as marked with arrow inset of Fig. 1(d), which shows the surface of Cu particles in a 0.4 3D disk electrode specimen. These small particles were also found at the surface of the Cu particles heated at 500°C for 2 h in N_2 (not shown in this manuscript).

The 3D disk electrodes operated well, as shown in Fig. 2, and the plateaus for both Cu₂O and CoO were observed. Moreover, at the first cycle, the ratio of Cu₂O plateaus was quite similar to the EPMA results, as seen in Fig. 2(a) and Table 2 [13,14]. At 0.1 3D

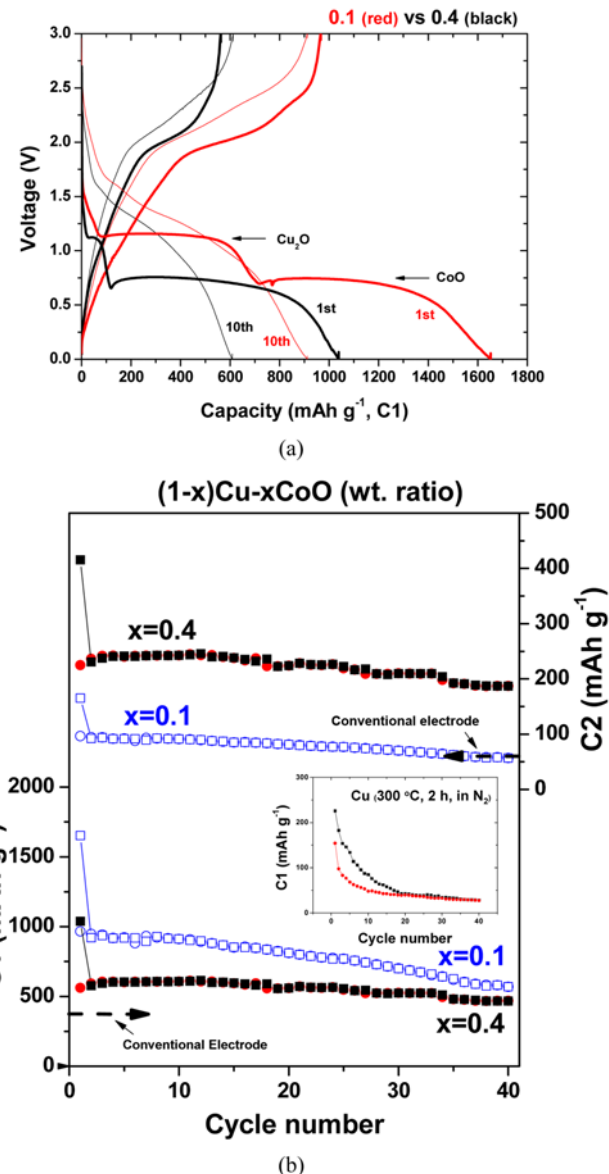


Fig. 2. (a) Charge and discharge curves and (b) cycling performances of 0.1 and 0.4 3D disk electrodes sintered at 500 and 600°C for 2 h.

disk electrode, a wider plateau of Cu₂O was observed, because a larger amount of Cu was oxidized compared to the 0.4 3D disk electrode. In addition, the 0.1 3D disk electrode showed higher C1 (1,650 and 970 mAh g⁻¹) than the 0.4 3D disk electrode (1,040 and 570 mAh g⁻¹) at the 1st cycle because of the higher Cu₂O ratio of 0.1 3D disk electrode. However, as shown in Fig. 2(b), better cycling retention was observed in the 0.4 than the 0.1 3D disk electrode. This better cycling performance of the 0.4 3D disk electrode might

Table 2. Cu oxidation rates of Cu and 3D disk electrodes (analyzed by EPMA)

Specimens	Ratio of Cu ₂ O [mol%/wt%]	Oxidation of Cu [mol%]	Sintering condition [°C, atmosphere]
Cu	72.9/85.8	72.9	500, N ₂
0.1 3D disk electrode	10.4/20.4	11.6	500, N ₂
0.4 3D disk electrode	3.0/6.2	5.0	600, N ₂

be due to the lower fraction of Cu₂O particles, which showed poor cycle retention as shown in the inset of Fig. 2(b). This poor cycle retention of small Cu₂O particles was already reported by Poizot et al. [14].

Primarily, 0.1 and 0.4 3D disk electrode specimens showed C2 of ~60 mAh g⁻¹ and ~190 mAh g⁻¹ at 40th cycle, respectively, as seen in Fig. 2(b). Therefore, it was demonstrated that the 0.4 3D disk electrode has excellent capacity, since F and C2 might be ~15 wt% and 107 mAh g⁻¹ in the conventional structure as seen at Table 1, when CoO was used for active material. In particular, the 0.4 3D disk electrode showed much higher capacity compared to the graphite-based conventional electrode. This means the electrode is also even lighter. Moreover, the CoO fraction was limited to approximately 40% in this work because of the size ratio (~0.3) as seen in Scheme 1(c) and Fig. 1(c). Therefore, further study can be focused on optimizing the structures of 3D disk electrodes. If smaller Cu particles (<34 nm) are used, the fraction must be enhanced to >90% and C2 can be also improved to >643 mAh g⁻¹ (11 times higher than conventional electrode as shown in Table 1). Furthermore, Cu coated CoO particle might be a more promising material for the 3D disk electrode. Therefore, the 3D disk electrode might be a promising candidate to improve energy density, etc., and reduce the weight in the electrode of the Li-ion battery.

ACKNOWLEDGEMENT

This work was supported by the National Research Foundation of Korea Grant funded by the Korean Government (MEST) (NRF-C1AAA001-2010-0029065). The authors gratefully acknowledge financial support from KIMS Internal Program “Development of Advanced Powder Materials Technology for New Growth Engine and Its Transfer to Industry.”

REFERENCES

1. M. Winter and J. O. Besenhard, *Electrochim. Acta*, **45**, 31 (1999).
2. Y. Idota, T. Kobota, A. Matsufuji, Y. Maekawa and T. Miyasaka, *Science*, **276**, 1395 (1997).
3. D. Larcher, A. S. Prakash, J. Saint, M. Mocrette and J.-M. Tarascon, *Chem. Mater.*, **16**, 5502 (2004).
4. J. Yang, B. F. Wang, K. Wang, Y. Liu, J. Y. Xie and Z. S. Wen, *Electrochim. Solid-State Lett.*, **6**(8), A154 (2003).
5. H. Bryngelsson, J. Eskhult, L. Nyholm, M. Herranen, O. Alm and K. Edström, *Chem. Mater.*, **19**, 1170 (2007).
6. S.-H. Ng, J. Wang, D. Wexler, K. Konstantinov, Z.-P. Guo and H.-K. Liu, *Angew. Chem. Int. Ed.*, **45**, 6869 (2006).
7. D. Larcher, S. Beattie, M. Morcrette, K. Edström, J.-C. Jumasc and J.-M. Tarascon, *J. Mater. Chem.*, **17**, 3759 (2007).
8. W. S. Kim, H. S. Kim, I. S. Park, Y. R. Kim, K. I. Chung, J. K. Lee and Y. E. Sung, *Electrochim. Acta*, **52**, 4566 (2007).
9. H. J. Ahn, Y. S. Kim, W. B. Kim, Y. E. Sung and T. Y. Seong, *J. Power Sources*, **163**(1), 211 (2006).
10. H. Li, P. Bayala and J. J. Maier, *Electrochim. Soc.*, **151**(11), A1878 (2004).
11. A. S. Arico, P. Bruce, B. Scrosati, J.-M. Tarascon and W. V. Schalkwijk, *Nature Mater.*, **4**, 366 (2005).
12. J. Chen, L. Xu, W. Li and X. Gou, *Adv. Mater.*, **17**, 582 (2005).
13. C. Q. Zhang, J. P. Tu, X. H. Huang, Y. F. Yuan, X. T. Chen and F. J. Mao, *Alloys Compd.*, **441**, 52 (2007).
14. P. Poizot, S. Laruelle, S. Grangeon, L. Dupont and J.-M. Tarascon, *Nature*, **407**, 496 (2000).
15. C. W. Ahn, H. C. Song, S. H. Park, S. Nahm, K. Uchino, S. Priya, H. G. Lee and N. K. Kang, *Jpn. J. Appl. Phys.*, **44**(3), 1314 (2005).
16. H. J. T. J. Ellingham, *Soc. Chem. Ind.*, **63**, 125 (1944).
17. D. R. Graskell, *Introduction to the thermodynamics of materials*, 3rd Ed., Taylor & Francis, Washington, 370 (1995).